

Isotopic Transient Study of La Promotion of Co/Al₂O₃ for CO Hydrogenation

Sturla Vada,¹ Bin Chen, and James G. Goodwin, Jr.²

Department of Chemical and Petroleum Engineering, University of Pittsburgh, Pittsburgh, Pennsylvania 15261

Received June 13, 1994; revised November 28, 1994

An investigation of La³⁺ promotion of 20 wt% Co/Al₂O₃ [(La/Co)_{atomic} = 0, 0.05, 0.10, and 1.0] for CO hydrogenation at 463–503 K and 1.8 atm has been carried out in order to develop a better understanding of the mechanism and effects of promotion. Chemisorption results show that at lower La³⁺ loadings there was a more significant effect on H₂ adsorption blockage. La³⁺ promotion enhanced the selectivity for higher hydrocarbons during CO hydrogenation, as has previously been observed for La³⁺-promoted Co catalysts at lower metal loadings, while the overall activity went through a maximum for La/Co = 0.05. Steady-state isotopic transient kinetic analysis (SSITKA) with carbon tracing was used to decouple the effects of La³⁺ on methane-producing sites during CO hydrogenation. The SSITKA results indicate that both a measure of the average methanation site/intermediate activity ($1/\tau_M$) and the concentration of active surface intermediates leading to CH₄ (N_M) increased upon initial La³⁺ promotion. At higher La³⁺ content the concentration of active surface intermediates leading to CH₄ decreased; however, the average site/intermediate activity remained essentially constant, resulting in a lower rate of methane formation. Deconvolution results indicate that La³⁺ promotion affected methane site activity by increasing the reactivity of the most active pool of intermediates. Increasing the H₂/CO inlet ratio at constant temperature and CO partial pressure led to an increase in the observed average site/intermediate activity, indicating a dependence on the concentration of surface hydrogen. One can conclude that while La³⁺ species block some of the Co surface, promotion results in the creation of more sites/intermediates on the surface having higher activities and probably results in a modification of the hydrogen surface concentration. © 1995 Academic Press, Inc.

INTRODUCTION

The development of active cobalt catalysts with high selectivity for long chain paraffins is of great importance for Fischer–Tropsch (F–T) processes for natural gas conversion. A Fischer–Tropsch catalyst for natural gas con-

version usually consists of four components: Co metal, a small amount of a second metal (usually noble), oxide promoters (alkali, rare earth, and/or a transition metal oxide such as ZrO₂), and a support (silica, alumina, or titania) (1).

Previous studies of rare earth oxide promotion have mainly focused on Ni-, Pd-, Rh-, Ru-, and Fe-based catalysts (2–8). Patent results suggest that rare earth promotion of Co is useful for Fischer–Tropsch synthesis (9–12). Barrault *et al.* (13) have shown that the addition of small amounts of La³⁺ to carbon-supported Co catalysts (prepared by coimpregnation) significantly increased the activity and the selectivity for higher hydrocarbons. Barrault *et al.* (14) have also studied CO hydrogenation on rare earth promoted Ni/C catalysts prepared by coimpregnation of aqueous solutions of nickel nitrate and lanthanum or cerium nitrate. They found that both the activity and selectivity to higher hydrocarbons and the selectivity to olefins increased upon promotion. Ledford *et al.* (15) found that low loadings of La³⁺ on a 10 wt% Co/alumina catalyst (La³⁺ impregnated before Co) had little effect on turnover frequency (TOF) for CO hydrogenation. However, a decrease in TOF was observed for higher La³⁺ loadings. They also found an increase in selectivity to C₂₊ and in olefin/paraffin ratio upon La³⁺ promotion. Wang *et al.* (16) studied the role of rare earth oxides and thoria as promoters in precipitated iron-based catalysts for F–T synthesis. They concluded that rare earth oxides and thoria have two functions. First, as structural promoters, they increase the dispersion and stabilization of the iron particles, inhibiting their growth and further reduction. Second, as chemical promoters, they encourage carbon monoxide adsorption, increase the probability of carbon monoxide dissociation by influencing the strength of the M–C and C–O bonds, and decrease the hydrogenation activity of the surface carbon species. Lanthanum promotion led to an increase in activity and selectivity to higher hydrocarbons.

The present study deals with the effect of La³⁺ on the behavior of alumina-supported cobalt catalysts. Steady-state isotopic transient kinetic analysis (SSITKA), devel-

¹ Present address: Department of Industrial Chemistry, Norwegian Institute of Technology, University of Trondheim, N-7034 Trondheim, Norway.

² To whom correspondence should be addressed.

oped in large part by Happel *et al.* (17) and Biloen *et al.* (18), was utilized to investigate how La^{3+} promotion affects $\text{Co}/\text{Al}_2\text{O}_3$ activity. By using SSITKA it is possible to separate the methanation rate into contributions from the concentration of active surface intermediates and contributions due to average site activity. From the SSITKA results for methane it is also possible to infer the effects of promotion on the synthesis of the other products.

EXPERIMENTAL

A $\gamma\text{-Al}_2\text{O}_3$ supported Co catalyst containing 20 wt% Co was prepared by impregnating $\gamma\text{-Al}_2\text{O}_3$ with an aqueous solution of $\text{Co}(\text{NO}_3)_2 \cdot 6\text{H}_2\text{O}$ using the incipient wetness technique. The catalyst precursor was dried for 10 h, calcined for 6 h at 573 K, and reduced for 22 h at 623 K after ramping at 1 K/min. After reduction, the catalyst was passivated by allowing air to leak slowly into the reduction system. The La^{3+} -promoted catalysts were prepared from this base, unpromoted catalyst in order to ensure similar Co particle size distributions. Portions of the reduced base catalyst were modified by impregnating them with an aqueous solution of $\text{La}(\text{NO}_3)_3 \cdot 5\text{H}_2\text{O}$ resulting in a series of catalysts with La/Co atomic ratios of 0.05, 0.10, and 1.00. The La/Co = 0.00 catalyst was prepared by impregnation with distilled water. These La^{3+} impregnation steps were followed by additional reduction under hydrogen at 623 K. In order to simplify notation, La/Co = 0, La/Co = 0.05, and La/Co = 0.10 catalysts are denoted in the subsequent discussion as LaCo.00, LaCo.05 and LaCo.10, respectively. The promoter is referred to as La^{3+} . Its exact compound form varies depending on the pretreatment and reaction conditions. Compounds such as $\text{La}_2(\text{CO}_3)_3$, $\text{La}(\text{OH})_3$, $\text{LaO}(\text{OH})_3$ (25), and, possibly, $\text{Co}(\text{LaO}_3)_x$ can exist, many concurrently.

The procedure used for the gas volumetric chemisorption was similar to that used by Reuel and Bartholomew (19). Static hydrogen rereduction was performed at 593 K for 10 h. Adsorption isotherms were measured at 298 K after initial equilibration at 373 K. The total adsorption isotherm was obtained by allowing a 60 min equilibration at each H_2 pressure. The number of total (reversible and irreversible) chemisorbed H atoms (extrapolated to zero pressure) was used to obtain the number of free Co atoms at the surface by assuming $\text{H}_{\text{total}}/\text{Co}_s = 1$, found to best correlate to the physical measurements (19).

CO hydrogenation at $\text{H}_2/\text{CO} = 10$ was carried out in a differential fixed-bed glass microreactor. The catalyst (30–60 mg) was rereduced in H_2 for 10 h at 623 K after ramping at 1 K/min, prior to reaction. The reaction was performed in the temperature range from 463 to 503 K at 1.8 atm. The feed composition was $\text{H}_2/\text{CO}/\text{He} = 20/2/78$

(ml/min). By using a H_2/CO ratio of 10, deactivation as a result of carbon deposition on the catalyst surface was minimized. Initial catalyst behavior was maintained by H_2 bracketing for 30 min between each reaction temperature. The product gases were analyzed using a Varian 3700 gas chromatograph equipped with FID and a 6-ft 60–80 mesh Poropak Q column.

The steady-state isotopic transient kinetic analysis (SSITKA) was also performed under the above-described conditions by switching $^{12}\text{CO}/^{13}\text{CO}$. A trace amount of argon was mixed in the ^{12}CO flow to permit determination of gas phase holdup. At 493 K the H_2/CO molar ratio was varied from 5 to 15 at constant CO partial pressure. The reaction was run for 5 min prior to an isotopic switch. The concentrations of Ar, ^{12}CO , ^{13}CO , $^{12}\text{CH}_4$, and $^{13}\text{CH}_4$ were continuously monitored during a switch by a Leybold–Inficon Auditor 2 mass spectrometer equipped with a high speed data acquisition system and controlled by an IBM-PC 386. By minimizing the dead volume in all tubing lines, the residence time of the trace gas (Ar) was shortened to less than 6 s.

The steady-state isotopic transient technique permits the monitoring of important kinetic parameters under steady-state reaction conditions. For methane formation the steady-state rate can be defined by

$$R_M = N_M/\tau_M, \quad [1]$$

where N_M is the surface concentration of intermediates which lead to CH_4 , and τ_M is the average surface residence time of the carbon in these reaction intermediates. SSITKA is able to determine both of these parameters and, thus, to deconvolute the reaction rate into contributions due to the concentration of reaction intermediates versus those due to the reactivity of these intermediates. The average pseudo-first-order intrinsic rate constant for CH_4 formation, k_M , corresponds to the inverse of the residence time of the surface reaction intermediates (τ_M), determined from steady-state isotopic transients, such as those shown in Fig. 6.

Usually, in the analysis of isotopic transients it is assumed that reaction takes place on a kinetically uniform catalyst surface. However, SSITKA can and has been extended for pseudo-first-order surface reactions to allow the assessment of surfaces that may not be kinetically uniform (20, 21). To investigate the effect that lanthanum may have had on different types of surface carbon, an extension of SSITKA (the F–T method) described elsewhere (21) was used for nonparametric determination of reactivity distribution functions, $f(k_M)$, from steady-state isotopic transients using a constrained standard Tikhonov regularization of the Fredholm equation of the first kind

$$R_M(t) = N_M \int k_M e^{-k_M t} f(k_M) dk_M, \quad [2]$$

TABLE 1
Properties of La-Promoted 20 Wt% Co/Al₂O₃ Catalysts (23)

La/Co (Atomic)	H_{total}^a ($\mu\text{mol/g}$)	Dispersion ^b (%)	Θ_{La}^c	CO conv. ^d (%)	R_{CO}^d ($\mu\text{mol/g/s}$)	CH ₄ Sel. ^d (%)	α , @ 483 K	
							H ₂ /CO = 2 ^e	H ₂ /CO = 10 ^d
0.00	193	5.7	0.0	4.3	1.00	52	0.57	0.41
0.05	167	4.9	0.13	4.7	1.84	46	0.74	—
0.10	130	3.8	0.33	2.8	0.60	42	0.70	0.46
1.00	91	2.7	0.53	—	—	—	—	—

^a From static hydrogen chemisorption at 373 K.

^b Based on assumption of $H_{\text{total}}/\text{Co}_s = 1$.

^c Estimated fraction of Co surface blocked by La species.

^d CO hydrogenation, $T = 483$ K, $P = 1.8$ atm, H₂/CO/He = 20/2/78 (ml/min).

^e CO hydrogenation, $T = 483$ K, $P = 1.0$ atm, H₂/CO = 33.7/16.3 (ml/min).

where $R_M(t)$ is the gas-phase-corrected steady-state isotopic transient of methane. The F-T method uses a variant on the approach suggested by Butler *et al.* (22) to determine the optimal amount of smoothing needed for integral inversion.

RESULTS

Table 1 gives the results from a preliminary study of these catalysts (23). The hydrogen chemisorption results were used to determine the amount of surface exposed Co, Co_s. The fraction of La³⁺-blocked cobalt surface atoms, Θ_{La} , was calculated by the fractional difference in Co_s of the particular catalyst with respect to the La-free catalyst. In addition, Table 1 gives the Fischer-Tropsch

chain growth probability, α , for these catalysts at 483 K for H₂/CO = 2 and 10. The chain growth probability was higher for the La³⁺-promoted catalysts at both H₂/CO ratios. The heavily promoted catalyst (La/Co = 1.0) had low activity for the F-T synthesis and consequently was not investigated further.

CO hydrogenation TOFs at different temperatures for the catalyst series are shown in Fig. 1. In order to compare initial catalyst properties and to minimize deactivation due to carbon deposition, H₂ bracketing between each reaction temperature and a high H₂/CO ratio of 10 were used. It can be seen that the TOF was highest for LaCo.05. The TOFs were approximately equal for the catalyst with the highest La³⁺ content (LaCo.10) and the unpromoted Co catalyst (LaCo.00).

Anderson-Schultz-Flory plots are shown in Figs. 2, 3, and 4 for LaCo.00, LaCo.05, and LaCo.10, respectively.

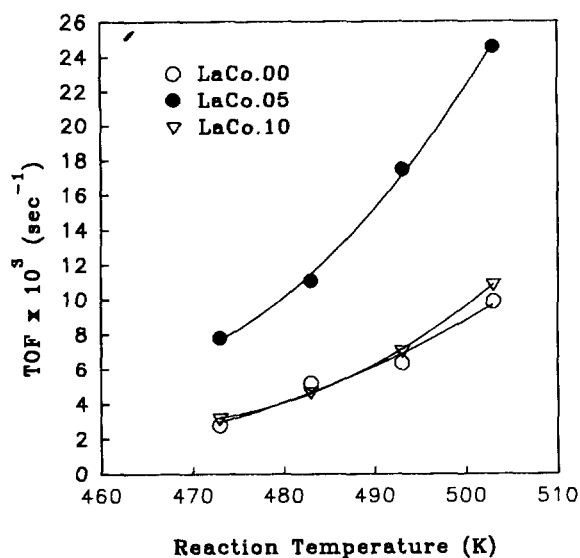


FIG. 1. Variation of overall turnover frequency (TOF) with reaction temperature for La³⁺-promoted Co catalysts (based on H₂ chemisorption).

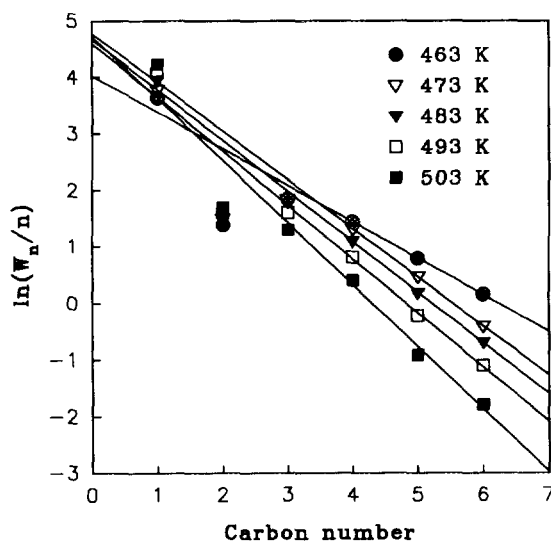


FIG. 2. Anderson-Schultz-Flory plots for LaCo.00.

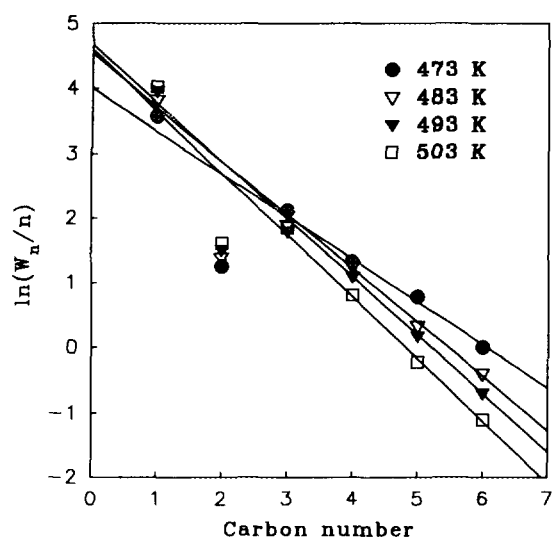


FIG. 3. Anderson-Schultz-Flory plots for LaCo.05.

It can be seen that the slope decreases with increasing temperature indicating a decrease in the chain growth probability, α . Such a decrease in α always occurs for an increase in temperature.

Arrhenius plots based on the rate of methane formation are displayed in Fig. 5. The activation energies for LaCo.00, LaCo.05, and LaCo.10 were found to be 110, 106, and 115 kJ/mol, respectively. The overall rate of methane formation was greatest on LaCo.05 and lowest on LaCo.10.

Steady-state isotopic transient kinetic analysis was used in this investigation in order to study in more detail what actually happens on the catalyst surface upon La^{3+} promotion. A typical normalized transient is shown in

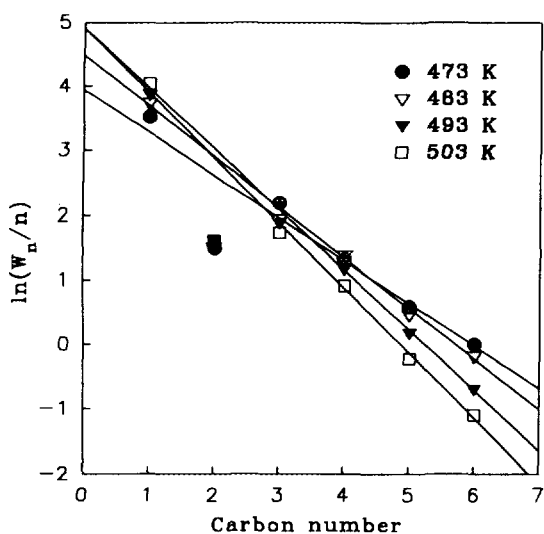


FIG. 4. Anderson-Schultz-Flory plots for LaCo.10.

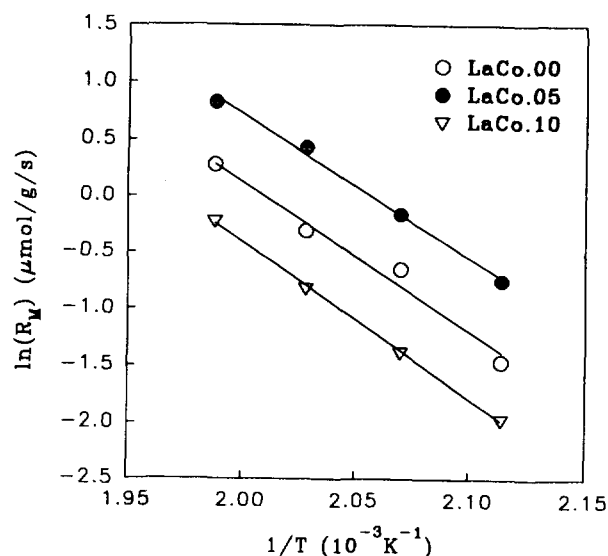


FIG. 5. Arrhenius plots for the rate of methane formation.

Fig. 6. The variations with temperature in the concentration of the active surface intermediates leading to methane (N_M) are shown in Fig. 7 for the various catalysts. N_M was highest for LaCo.05. However, the catalyst with the highest La^{3+} content had the lowest concentration of surface intermediates. N_M increased significantly with temperature for all the catalysts.

SSITKA results for different H_2/CO inlet ratios for LaCo.00, LaCo.05, and LaCo.10 are shown in Table 2. The partial pressure of CO was kept constant at all ratios. It can be seen that overall rate and TOF were highest for

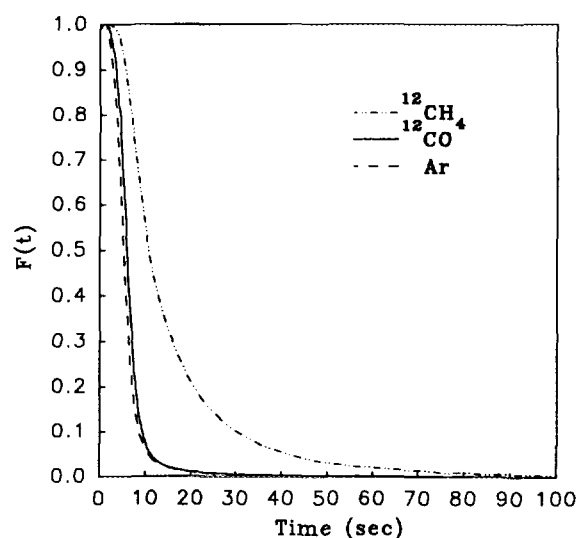


FIG. 6. Isotopic transients of Ar, ^{12}CO , and $^{12}\text{CH}_4$ corresponding to a switch from ^{12}CO to ^{13}CO (catalyst: LaCo.10, $T = 493\text{ K}$). $F_j(t)$ is the fraction of the labeled j th species in the reactor effluent [$F_j(0) = 1$ at the time of the isotopic switch].

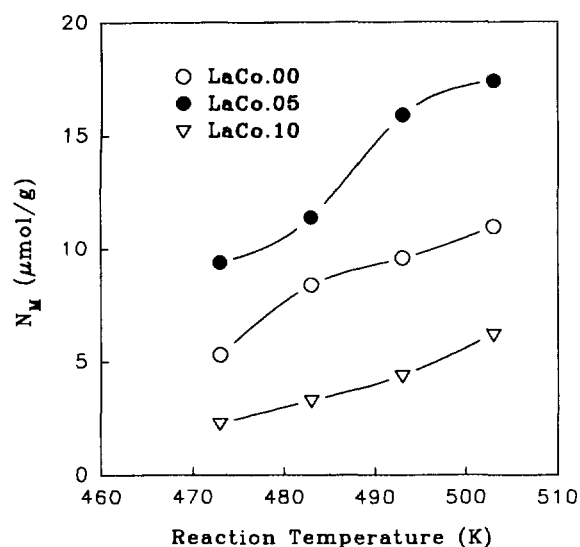


FIG. 7. Variation of the concentration of active surface intermediates, N_M , with reaction temperature.

La/Co = 0.05 at all H_2/CO ratios. The average surface residence time, τ_M , decreased with increasing H_2/CO ratio for all catalysts, while the coverage of surface intermediates which led to methane (Θ_M) and the coverage of CO (Θ_{CO}) remained essentially constant for each of the catalysts.

DISCUSSION

The chemisorption results show that blocking of Co sites by La^{3+} occurred upon promotion (Table 1). This was also confirmed by a decrease in ethane hydrogenoly-

sis activity (23). The nonlinear relationship between La/Co atomic ratio and the amount of total chemisorbed hydrogen indicates that La^{3+} had a greater impact on H_2 chemisorption for the lowest La^{3+} loadings. In any case, the initial small loadings of La^{3+} probably had a larger impact on chemisorption due to the preferential siting of La^{3+} on the Co surface. Additional amounts were probably distributed between the Co and support surfaces, with the Co surface approaching a saturation point. This is also seen for Co/ SiO_2 (26). What actually happens on the cobalt surface is not known for certain, but there is some evidence that La^{3+} may not just be sitting on the surface blocking sites. It has been suggested that there is a reaction between Co and La^{3+} to form mixed Co-La oxides (15), the nature of which has not yet been successfully determined.

The chain growth probability was higher for La^{3+} -promoted catalyst at both ratios. Ledford *et al.* (15) did not observe any promotion effect of La^{3+} for CO hydrogenation on catalysts prepared by impregnation of La^{3+} onto Co/ Al_2O_3 . However, the La^{3+} -promoted catalyst used in the experiments reported here were calcined, reduced, and passivated prior to La^{3+} -impregnation, while Ledford *et al.* (15) only calcined the Co catalyst before the impregnation of La^{3+} . It is surmised that the state of Co during La^{3+} impregnation affects its distribution on the catalyst surface resulting in more or less promoting effects. An elaboration as to how this works requires more research to avoid sheer speculation.

The specific activity (TOF) was highest for LaCo.05 (Fig. 1). The concentration of surface intermediates which led to CH_4 (N_M) was also highest for this catalyst (Fig. 7). However, based on the hydrogen chemisorption

TABLE 2

SSITKA Results for CO Hydrogenation on La^{3+} Promoted Co/ Al_2O_3 at Different H_2/CO Inlet Ratios ($T = 493 \text{ K}$)^a

H_2/CO (inlet)	R_{CO} ($\mu\text{mol/g/s}$)	TOF $\times 10^3$ ^b (s^{-1})	CH_4 Sel. (%)	τ_{CO} (s)	τ_M^c (s)	N_{CO} ($\mu\text{mol/g}$)	N_M^c ($\mu\text{mol/g}$)	Θ_{CO}^b	$\Theta_M^{b,c}$
LaCo.00									
5	0.63	3.3	51	0.9	29.2	20.9	9.3	0.11	0.05
10	1.23	6.4	59	1.0	13.0	23.9	9.6	0.12	0.05
15	1.71	8.9	64	0.9	7.1	21.2	7.8	0.11	0.04
LaCo.05									
5	1.49	9.0	46	1.0	16.6	37.8	11.4	0.23	0.07
10	2.90	17.5	53	0.8	10.3	29.1	15.9	0.18	0.10
15	3.61	21.7	57	0.9	6.2	32.1	12.8	0.19	0.08
LaCo.10									
5	0.49	3.8	38	0.8	18.8	16.9	3.5	0.13	0.03
10	0.92	7.1	48	0.7	10.0	14.0	4.4	0.11	0.03
15	1.28	9.9	53	0.6	7.6	12.6	5.2	0.10	0.04

^a H_2 bracketing in between reaction at each ratio. $\text{Flow}_{\text{CO}} = 2 \text{ ml/min}$, total flow = 100 ml/min, total pressure = 1.8 atm.

^b Based on hydrogen chemisorption.

^c Intermediates leading to CH_4 .

results, the amount of surface exposed Co decreased upon La^{3+} promotion. The pseudo-first-order rate constant for methane formation ($1/\tau_M$) did not change much upon La^{3+} promotion (Fig. 8). However, it seems that $1/\tau_M$ was slightly greater for both promoted catalysts compared to the unpromoted catalyst at all reaction temperatures. Therefore, these SSITKA results clearly show that blocking of Co sites was not the only effect of La^{3+} on the catalyst surface upon promotion. Three explanations exist for why the LaCo.05 catalyst gave higher overall activity. One possibility is that La^{3+} interacted in some way with Co to form new highly active sites. Another possibility is that the concentration of surface intermediates, N_i , increased. A third possibility is that a combination of the two aforementioned statements occurred. However, since both the average $k_M(1/\tau_M)$ and N_M were greater for the LaCo.05 catalyst, at least for the formation of methane, we suggest that both effects occur for this catalyst upon La^{3+} promotion. At higher La^{3+} content (LaCo.10), N_M decreased and was even lower than for the unpromoted catalyst. We suggest, therefore, that the blockage effect was more pronounced for higher La^{3+} contents.

Arrhenius plots based on $1/\tau_M$ are displayed in Fig. 8. The apparent activation energies of $1/\tau_M$ for LaCo.00, LaCo.05, and LaCo.10 were determined to be 64, 63, and 50 kJ/mol, respectively. Figure 8 also shows that $1/\tau_M$ was enhanced upon La promotion. The activation energies determined from the rate of methane formation, R_M , are in good agreement with those reported in the literature. However, the activation energies determined from $1/\tau_M$ are lower than the activation energies determined from R_M . This difference exists due to the assumption

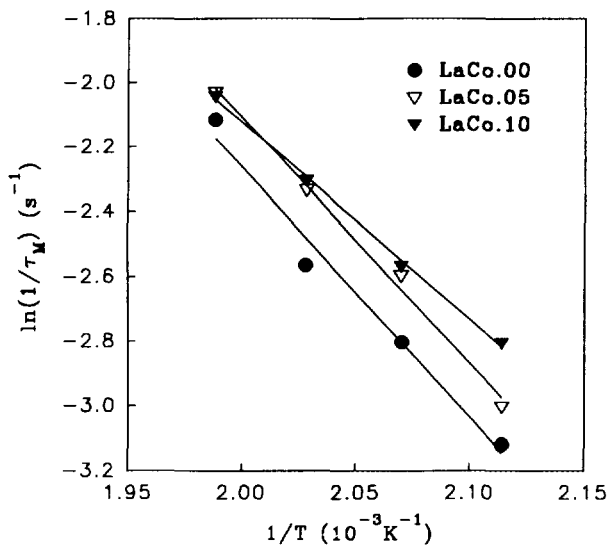


FIG. 8. Arrhenius plots for $1/\tau_M$.

that R_M was dependent only on the reaction temperature. This was not the case (Fig. 7) since the concentration of surface intermediates of methane (N_M) increased with reaction temperature.

The reactivity distributions for methane formation ($f(k_M)$ in Eq. [2]) for this series of La^{3+} -promoted catalysts are displayed in Fig. 9. The distribution function has been weighted by the concentration of surface intermediates of methane so that not only activity changes are seen but also total concentration of sites. Figure 9 shows that the formation of methane on this series of La^{3+} -promoted catalysts was regulated by two reaction pathways for methane-destined surface intermediates. As can be seen in Fig. 9, promotion of Co with La^{3+} affected primarily the pool with highest activity. In addition, peak location did not change for the higher level of La^{3+} promotion, indicating no change in site activity (k). These results are in agreement with the results determined from the average $k_M(1/\tau_M)$.

Upon increasing H_2/CO inlet ratio, the average surface residence time τ_M decreased (Table 2). This decrease in τ_M indicates that the pseudo-first-order rate constant (k_M) increased with increasing H_2/CO inlet ratio at constant

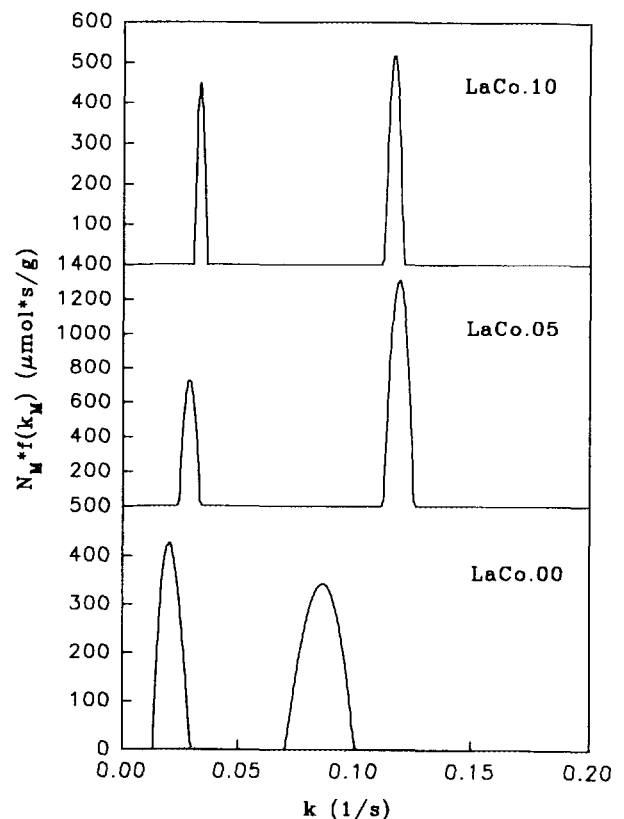


FIG. 9. Reactivity distribution obtained by SSITKA of methane-destined carbon during F-T synthesis at 493 K, 1.8 atm, and $\text{H}_2/\text{CO} = 10$.

reaction temperature since k_M is proportional to $1/\tau_M$. Obviously, a true rate constant should be only a function of reaction temperature. To explain this effect it is important to note that the overall rate of methane formation, based on the rate-determining step being the hydrogenation of surface intermediates (the case generally for Co), can be expressed as

$$R_M = (k_M)_{\text{true}} \cdot N_H \cdot N_M, \quad [3]$$

where $(k_M)_{\text{true}}$ is the true rate constant for methane formation, N_H is the surface concentration of hydrogen, and N_M is the surface concentration of carbon-based species which lead to methane. However, since we are not able to determine N_H , the calculated k_M is related to the true rate constant by

$$k_M = (k_M)_{\text{true}} \cdot N_H = \frac{1}{\tau_M}. \quad [4]$$

Thus, an increase in k_M ($1/\tau_M$) with an increase in H_2/CO ratio would be due to the fact that N_H , the surface concentration in H, increased. Unfortunately, due to isotope effects during H_2/D_2 switching, N_H cannot be determined exactly by SSITKA. However, by dividing $1/\tau_M$ for a given H_2/CO ratio by the value for it at a reference ratio ($H_2/CO = 5$)

$$\frac{(1/\tau_M)_i}{(1/\tau_M)_5} = \frac{(k_M)_{\text{true}}(N_H)_i}{(k_M)_{\text{true}}(N_H)_5} = \frac{(N_H)_i}{(N_H)_5}, \quad [5]$$

a measure of the relative variation in the surface concentration of hydrogen with H_2/CO ratio can be determined. A plot of the surface concentration of adsorbed hydrogen relative to that at $H_2/CO = 5$ versus the H_2/CO inlet ratio is shown in Fig. 10. It is seen that the relative amount of H adsorbed increased upon increasing this ratio. This is one reason why the rate of methane formation increased upon increasing the H_2/CO inlet ratio, since both the coverage of CO and the coverage of methane-destined surface intermediates remained essentially constant (Table 2). The amount of reactive hydrogen increased by a factor of approximately 2.5 upon increasing the H_2/CO ratio from 5 to 15. Zhang and Biloen (24) performed essentially the same kind of experiments for a precipitated Co catalyst. They changed the D_2/CO ratio from 1 to 7 (at 483 K and 1 bar) but found little variation in the average lifetime of the surface intermediates, which they found surprising. It is possible that the differences observed were due to the effect of changing the H_2/CO ratio from 5 to 15 instead of from 1 to 7, to the isotope effect of D_2 , or to differently prepared Co catalysts. A conclusion cannot be made at this time based on the experimental results.

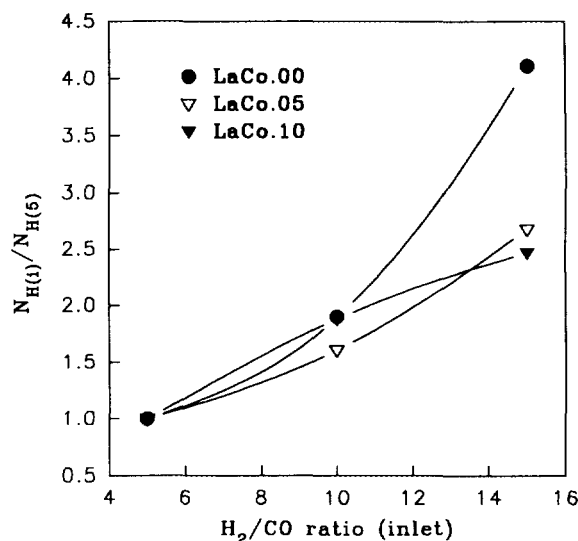


FIG. 10. Relative concentration of active hydrogen on the catalyst surface as a function of H_2/CO ratio i .

CONCLUSIONS

Hydrogen chemisorption on Co/Al_2O_3 was significantly blocked with increasing La^{3+} loading. La^{3+} promotion increased the selectivity for heavier hydrocarbons during CO hydrogenation. Such results are similar to those which others have previously observed at lower Co contents. While the overall catalyst activity increased for a low La^{3+} loading ($La/Co = 0.05$), it decreased for the higher loadings studied (≥ 0.10). Steady-state isotopic transient kinetic analysis results indicate that both the average site activity (as measured by $1/\tau_M$) and the concentration of active surface intermediates leading to CH_4 (N_M) increased for the lowest level of La^{3+} promotion ($La/Co = 0.05$). However, at higher La^{3+} content the concentration of active surface intermediates leading to CH_4 decreased, while the average site/intermediate activity remained essentially constant, resulting in a lower rate of methane formation. The deconvolution results indicate that the methane-destined surface intermediates mainly fall into two pools and that the reactivity of the high activity pool is enhanced by La^{3+} promotion. These results are in agreement with the results determined from the average k_M ($1/\tau_M$). Upon increasing the H_2/CO inlet ratio at constant temperature, the observed average site/intermediate activity increased. It was shown that this increase was due to the increased concentration of surface hydrogen. The concentration of surface hydrogen increased by a factor of 2.5 for the La^{3+} -promoted catalysts upon increasing the H_2/CO inlet ratio from 5 to 15. The increase was even greater for the unpromoted catalyst. The effect of La^{3+} promotion on hydrogen surface coverage during CO hydrogenation is probably a factor in increasing the chain growth probability.

ACKNOWLEDGMENTS

S. Vada thanks the Norwegian Institute of Technology and Royal Norwegian Council for Scientific and Industrial Research for funding his stay at the University of Pittsburgh. The authors thank the National Science Foundation (Grant CTS-9102960) and Amoco Oil Co. for financial support.

REFERENCES

1. Goodwin, J. G., Jr., *Prepr. Am. Chem. Soc. Div. Petr. Chem.* **36**, 156 (1991).
2. Fleisch, T. H., Hicks, R. F., and Bell, A. T., *J. Catal.* **87**, 398 (1984).
3. Rieck, J. S., and Bell, A. T., *J. Catal.* **96**, 88 (1985).
4. Chen, Y. W., and Goodwin, J. G., Jr., *React. Kinet. Catal. Lett.* **26**, 453 (1984).
5. Gelsthorpe, M. R., Mok, K. B., Ross, J. R. H., and Sambrook, R. M., *J. Mol. Catal.* **25**, 253 (1984).
6. Kieffer, R., Kiennemann, A., Rodriguez, M., Bernal, S., and Rodriguez-Izquierdo, J. M., *Appl. Catal.* **42**, 77 (1988).
7. Schaper, H., Doesburg, E. B. M., de Korte, P. H. M., and van Reijen, L. L., *Appl. Catal.* **14**, 371 (1985).
8. Baker, B. G., and Clark, N. J., *Stud. Surf. Sci. Catal.* **31**, 455 (1987).
9. Eri, S., Goodwin, J. G., Jr., Marcelin, G., and Riis, T., U. S. Patent 4,801,573, 1989.
10. Beuther, H., Kibby, C. L., Kobylinski, T. P., and Pannell, R. B., U. S. Patent 4,399,234, Aug. 16, 1983 and U. S. Patent 4,413,064, Nov. 1, 1983.
11. Kibby, C. L., and Kobylinski, T. P., U. S. Patent 4,497,903, Feb. 5, 1985.
12. Beuther, H., Kibby, C. L., Kobylinski, T. P., and Pannell, R. B., U. S. Patent 4,613,624, Sept. 23, 1986 and U. S. Patent 4,605,680, Aug. 12, 1986.
13. Barrault, J., Guilleminot, A., Achard, J., Paul-Boncour, V., and Percheron-Guegan, *Appl. Catal.* **21**, 307 (1986).
14. Barrault, J., Chafik, A., and Gallezot, P., *Appl. Catal.* **67**, 257 (1991).
15. Ledford, J. S., Houalla, M., Proctor, A., Hercules, D. M., and Petrakis, L., *J. Phys. Chem.* **93**, 6770 (1989).
16. Wang, D., Cheng, X., Huang, Z., Wang, X., and Peng, S., *Appl. Catal.* **77**, 109 (1991).
17. Happel, J., Suzuki, I., Kokayeff, P., and Fthenakis, V., *J. Catal.* **65**, 59 (1980).
18. Biloen, P., Helle, J. N., van den Berg, F. G. A., and Sachtler, W. M. H., *J. Catal.* **81**, 450 (1983).
19. Reuel, R. C., and Bartholomew, C. H., *J. Catal.* **85**, 63 (1984).
20. de Pontes, M., Yokomizo, G. H., and Bell, A. T., *J. Catal.* **104**, 147 (1987).
21. Hoost, T. E., and Goodwin, J. G., Jr., *J. Catal.* **134**, 678 (1992).
22. Butler, J. P., Reeds, J. A., and Dawson, S. V., *SIAM J. Numer. Anal.* **18**, 381 (1981).
23. Vada, S., Chen, B., Kazi, A. M., Bedu-Addo, F. K., and Goodwin, J. G., Jr., *Stud. Surf. Sci. Catal.* **81**, 443 (1994).
24. Zhang, X., and Biloen, P., *J. Catal.* **98**, 468 (1986).
25. Gallaher, G., Goodwin, J. G., Jr., Huang, C.-S., and Houalla, M., *J. Catal.* **127**, 719 (1991).
26. Haddad, G., Chen, B., and Goodwin, J. G., Jr., submitted for publication.